ORIGINAL RESEARCH

The A150V Polymorphism of Genotype 3 Hepatitis C Virus Polymerase Inhibits Interferon Alfa by Suppressing Protein Kinase R Activation

Wing-Yiu Jason Lee,[1] Meleri Jones,[1] Peter A. C. Wing,[2] Swathi Rajagopal,[1] and Graham R. Foster[1]

[1]Centre of Immunobiology, Blizard Institute, Queen Mary University of London, London; and [2]Nuffield Department of Medicine, University of Oxford, Oxford, United Kingdom

SUMMARY

A polymorphism in the genotype 3 HCV polymerase (A150V) known to reduce response to sofosbuvir reduced the antiviral effect of interferon alpha. Despite intact IFN-mediated signaling and induction of interferon-stimulated genes, A150V perturbed activation of PKR, nuclear localization of activated PKR, and concomitant induction of apoptosis.

BACKGROUND & AIMS: Despite recent advances in antiviral therapy for hepatitis C virus (HCV), a proportion of patients with genotype 3 (G3) HCV infection do not respond to current all oral treatment regimens. Genomic analyses have identified key polymorphisms correlating with increased resistance to direct-acting antivirals. We previously reported that amino the acid polymorphism, A150V, in the polymerase (NS5B) of G3 HCV reduces response to sofosbuvir. We now demonstrate that this polymorphism alters the response to interferon alpha.

METHODS: Quantitative polymerase chain reaction, immunofluorescence, luciferase activity assay, immunoblotting, and flow cytometry were used to study the antiviral effect of interferon (IFN) on DBN G3 HCV-infected cells and G3 HCV replicons.

RESULTS: We show the presence of the A150V polymorphism markedly reduces the response to IFN alpha (IC$_{50}$ of S52_WT = 1.162 IU/mL and IC$_{50}$ of S52_A150V = 14.45 IU/mL, 12.4-fold difference). The induction of IFN-stimulated genes in A150V replicon cells is unaffected, but nuclear localization of active protein kinase R (PKR) is reduced. Blockade of PKR activity reduced the antiviral effect of IFN on wild-type replicons, whereas augmented PKR activation promoted the antiviral effect of IFN on A150V replicons. Furthermore, we show that impaired activation of PKR in A150V replicon cells diminishes cellular apoptosis.

CONCLUSIONS: These results demonstrate that polymorphisms reducing response rates to direct-acting antivirals may function beyond conferring drug resistance by modulating the intrinsic cellular antiviral response. *(Cell Mol Gastroenterol Hepatol 2021;11:1163–1175; https://doi.org/10.1016/j.jcmgh.2020.11.012)*

Keywords: Hepatitis C Virus; Interferon; Protein Kinase R; Viral Replication; Apoptosis.

Chronic infection with the hepatitis C virus (HCV) affects at least 70 million people worldwide,[1] causing cirrhosis and hepatocellular carcinoma in a large proportion of those infected.[2] Despite recent advances in antiviral therapy for HCV, a proportion of patients with genotype 3 (G3) HCV infection do not respond to current all oral treatment regimens.[3,4] Previously a combination of pegylated interferon (IFN) and ribavirin, a nucleoside analogue, was the gold standard of therapy for HCV, yet response rates were variable, with a low proportion achieving a sustained virologic response.[5–11] Over the last few years treatment for HCV has moved from IFN-based regimens to more effective, better tolerated direct-acting antiviral agents.[12] The backbone of many of these regimens is the nucleotide analogue sofosbuvir, which has activity against all HCV genotypes and, in combination with the pan-genotypic NS5A inhibitor velpatasvir, eliminates the virus in more than 90% of patients.[13] However, sofosbuvir-based regimens have reduced efficacy in cirrhotic patients with G3 HCV, leading to suggestions that such patients should receive augmented treatment with sofosbuvir/velpatasvir and the protease inhibitor voxilaprevir.[14]

Interestingly, response to all oral regimens is further reduced in G3 HCV patients previously treated with IFN. A genetic association study of patients treated with sofosbuvir identified a viral polymorphism in the polymerase at amino acid position 150 that was linked to the IFN lambda gene cluster.[15] Our previous work discovered and

Most current article

characterized a number of substitutions in G3 HCV NS5B,[16] which reduced the response to sofosbuvir. One of these substitutions (A150V) was also identified in a gene association study potentially linking IFN response to sofosbuvir sensitivity.[15] Because of the link between IFN treatment failure and reduced response to sofosbuvir along with the genomic association, we speculated that common polymorphisms in G3 HCV might affect response to both sofosbuvir and IFN.

Type I IFNs signal via phosphorylation of STAT1/2 and activation of IRF9 to drive the expression of IFN-stimulated genes (ISGs) for suppression of HCV replication.[17] Protein kinase R (PKR) is one of the ISGs transcriptionally activated by IFN. Double-stranded RNA (dsRNA), generated as a result of viral replication, interacts with the dsRNA binding domain of PKR, causing a conformational change leading to dimerization and autophosphorylation of the kinase domain for subsequent phosphorylation of targets such as eukaryotic initiation factor 2α (EIF2α).[18] Interestingly, people with polymorphisms in the promoter region of PKR, resulting in perturbed activity, succumb more severely to HCV infections.[19] The internal ribosome entry site in the 5'-untranslated region of HCV RNA binds to and induces autophosphorylation of PKR.[20] Activated PKR suppresses HCV replication in the context of IFNα via hyperphosphorylation of EIF2α and concomitant translational suppression of ISGs. Interferon resistance of HCV infections has been associated with adaptive mutations in the IFN sensitivity determining region of NS5A.[21–23] More recently, the RNA-dependent RNA polymerase, NS5B of genotype 2 HCV, JFH1, has been shown to interact with and activate PKR to modulate MHC-I expression on cell surface,[24] suggesting that there is an interaction between HCV and IFN inducible antiviral proteins.

Here we assess the effects of the A150V polymorphism on response to IFN and show that this polymorphism perturbs activation of the downstream IFN effector protein PKR.

Results

The A150V Polymorphism Reduces the Antiviral Effect of IFN

To assess the impact of the A150V polymorphism on the replication of HCV we introduced this polymorphism into cell culture derived G3 virus.[16] There was no significant difference in infectivity (Figure 1A) of the 2 viruses, confirming our previous viral fitness comparison between wild-type (WT) and A150V viruses.[16] Infection of Huh7.5 cells with these viruses followed by treatment with a range of IFNα2a doses resulted in a significant loss in sensitivity to IFN in the A150V virus compared with WT, assessed by HCV RNA (Figure 1B) and quantification of HCV NS5A immunofluorescence in infected cells (Figure 1C). We confirmed this observation in cells expressing subgenomic G3 replicons where luciferase activity correlates with the extent of replication.[16,25] Titration of IFNα2a (Figure 1D) on WT or A150V replicons resulted in 12-fold increase in IC$_{50}$ in A150V replicon cells compared with WT, highlighting that presence of the A150V polymorphism significantly reduces sensitivity to IFN.

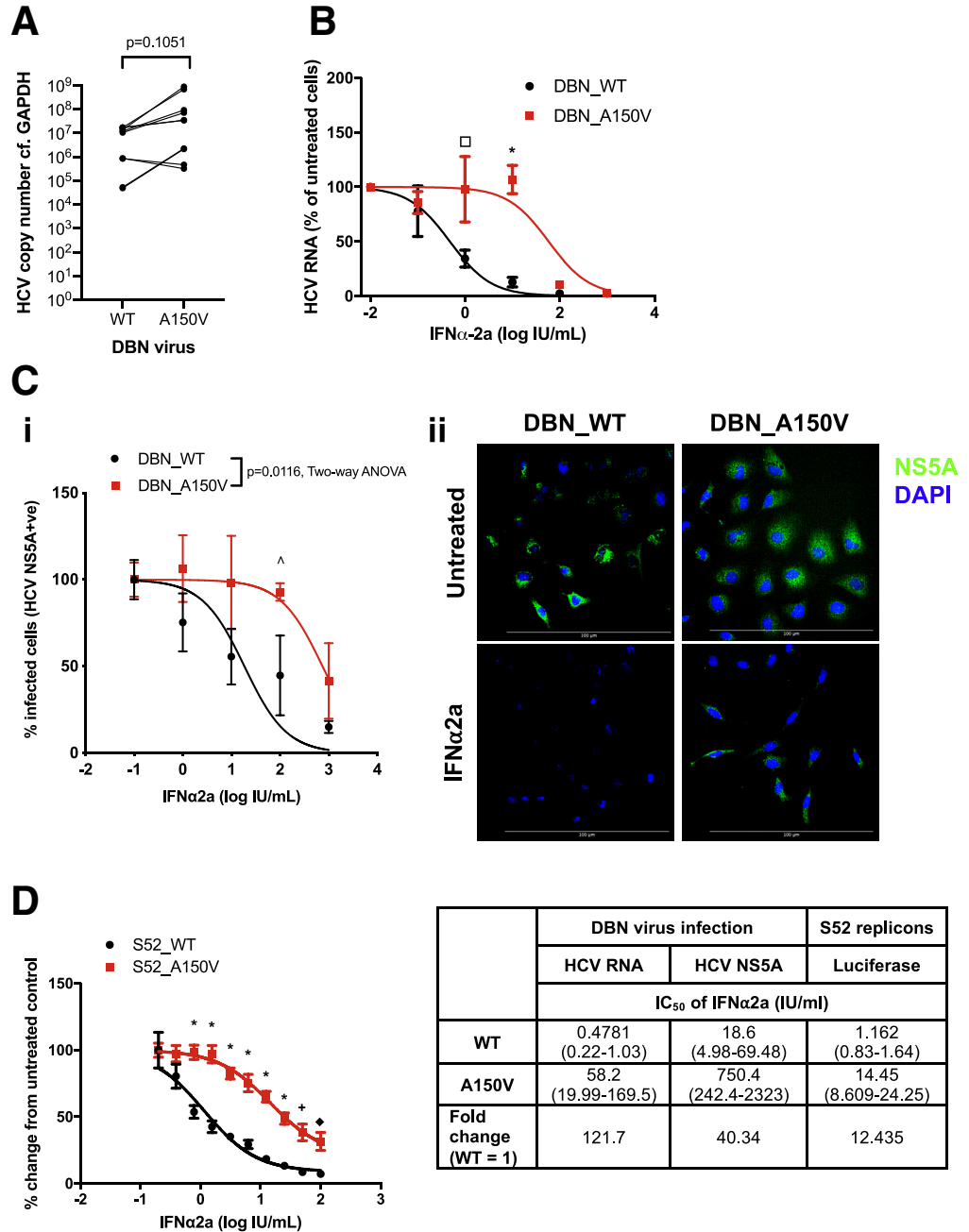### A150V Replicon Does not Affect Proximal IFN Signaling and ISG Transcriptional Activation

Type I IFN signals via activation of the JAK/STAT signaling pathway, resulting in a complex between STAT1/2 and IRF9 (interferon-stimulated factor 3 [ISGF3]) that drives expression of ISGs. This establishes an antiviral state resulting in a positive feedback loop with further expression of STAT1 activating a pathway based on unphosphorylated ISGF3.[26] To understand how a single amino acid polymorphism in NS5B could cause an increase in IFN resistance, we assessed the proximal signaling pathway in replicon cells 6 hours after IFN treatment by immunoblotting (Figure 2A). The level of phospho-STAT-1 in replicon-containing cells upon IFN treatment was slightly higher than in the parental cell line, whereas there was no significant difference between WT and A150V replicons (Figure 2B). We also confirmed that the block of IFN-mediated antiviral effect is not due to a reduction in STAT2 expression or activation (Figure 2A and B). In addition, there was no significant difference in IFN-induced total STAT-1 in all cell lines. Next we analyzed the induction of a selection of ISG transcripts known to be regulated by unphosphorylated ISGF3 (MxA and OAS1) and ISGF3 (ADAR, MyD88, and PKR)[26] by reverse transcriptase quantitative polymerase chain reaction (RT-qPCR) and found no significant difference between WT and A150V replicons (Figure 2C). Collectively, these data suggest that A150V containing HCV replicons do not affect proximal IFN signal transduction or the downstream transcriptional induction of ISGs.

PKR Activation Is Induced in Replicons but It Is Repressed by A150V

Because we observed no perturbation of the IFN signaling pathway, we hypothesized that the A150V polymorphism may act downstream of ISG induction to mediate resistance to IFN. We tested whether PKR plays a role in detecting and controlling viral replication in our replicon system. Quantitative PCR verified that IFN induced up-regulation of PKR mRNA in Huh7.5 cells with and without replicons (Figure 2C). Activation of PKR protein was assessed by immunoblotting using antibodies against unphosphorylated and phosphorylated protein (antibody specific for the phosphorylated tyrosine residue 446[27]) 6 hours after IFN treatment (Figure 3A and B). As expected from the mRNA experiments, IFN induced total PKR expression in both parental Huh7.5-SEC14L2 and replicon-containing cells. Cells containing the WT HCV replicon showed an increase in PKR phosphorylation upon IFN treatment in the presence of replicating virus, shown as the ratio of phosphorylated PKR to total PKR. However, in cells containing the A150V replicon, there was no increase in the ratio of phosphorylated PKR to total PKR upon IFN treatment, indicating a defect in PKR activation (Figure 3A and B). Because of the pleiotropic effects of IFN treatment we assessed PKR activation using poly-I:C, a synthetic ligand of PKR. We demonstrated that poly I:C treatment increased

Figure 1. IFN resistance in HCV G3 A150V replicon and HCV-A150V infected Huh7.5 cells. (A) Huh7.5-SEC14L2 cells were infected with indicated G3 DBN viruses at multiplicity of infection of 0.2 for 8 days before RT-qPCR analysis of HCV viral copy. Infected cells were re-plated 24 hours before treatment with serial dilutions of IFNα2a. At 72 hours after treatment with IFNα2a, (B) level of HCV RNA was quantified by RT-qPCR, (Ci) percentage of infection with NS5A immunofluorescence was quantified with IN Cell automated microscopy, and representative images are shown (Cii). Data show mean + SEM normalized to untreated control. (D) Huh7.5-DBNS52 WT (black) and A150V (red) replicon cells were treated with IFNα2a for 72 hours and then quantified for luciferase activity. Table shows IC$_{50}$ of IFNα2a and the fold difference between WT and A150V. Data show mean + SEM normalized to untreated controls from at least 3 independent experiments. *$P <$ .0001, +$P =$ .0011, ^$P =$ .05, ◆$P =$ .0116, and □$P =$ .0067 by 2-way analysis of variance and mixed effect analysis.

	DBN virus infection		S52 replicons
	HCV RNA	**HCV NS5A**	**Luciferase**
	IC$_{50}$ of IFNα2a (IU/ml)		
WT	0.4781 (0.22-1.03)	18.6 (4.98-69.48)	1.162 (0.83-1.64)
A150V	58.2 (19.99-169.5)	750.4 (242.4-2323)	14.45 (8.609-24.25)
Fold change (WT = 1)	121.7	40.34	12.435

PKR phosphorylation, as previously reported,[28] in parental Huh7.5 cells, and this activation could be inhibited by the PKR phosphorylation inhibitor 2-aminopurine (2-AP) (Figure 3C). Poly-I:C treatment significantly induced phosphorylated PKR in WT replicon cells, yet no up-regulation was observed in A150V replicon cells (Figure 3C and D).

To determine whether the A150V polymorphism in NS5B in isolation is responsible for the inhibitory effect of PKR activation, we analyzed dsRNA-induced PKR phosphorylation in Huh7 cells stably expressing either WT or A150V G3 NS5B (Figure 4A) in the absence of other hepatitis C viral proteins. Poly-I:C treatment of parental Huh7

cells induced PKR activation, yet cells stably expressing either WT or A150V G3-NS5B appeared to have markedly reduced induction of phosphorylated PKR (Figure 4B), suggesting that NS5B in isolation perturbs PKR activation in response to dsRNA. The A150V polymorphism is located in the region of NS5B thought to interact with NS5A,[16] and because NS5A may sequester NS5B within the replicating virus, we hypothesized that the A150V polymorphism in the NS5B-NS5A interaction interface promotes the NS5B interaction with PKR, perhaps by increased access of PKR to NS5B, and facilitates inhibition. We tested this hypothesis by using quantitative immunofluorescence of replicating virus

(detected by NS5A staining) and phosphorylated PKR in the replicon cells with and without IFN treatment. Similar to previous findings, the level of phospho-PKR was higher in

WT replicons compared with parental Huh7.5 and was further increased upon IFN treatment (Figure 4C and D). The basal level of phospho-PKR in A150V replicon was
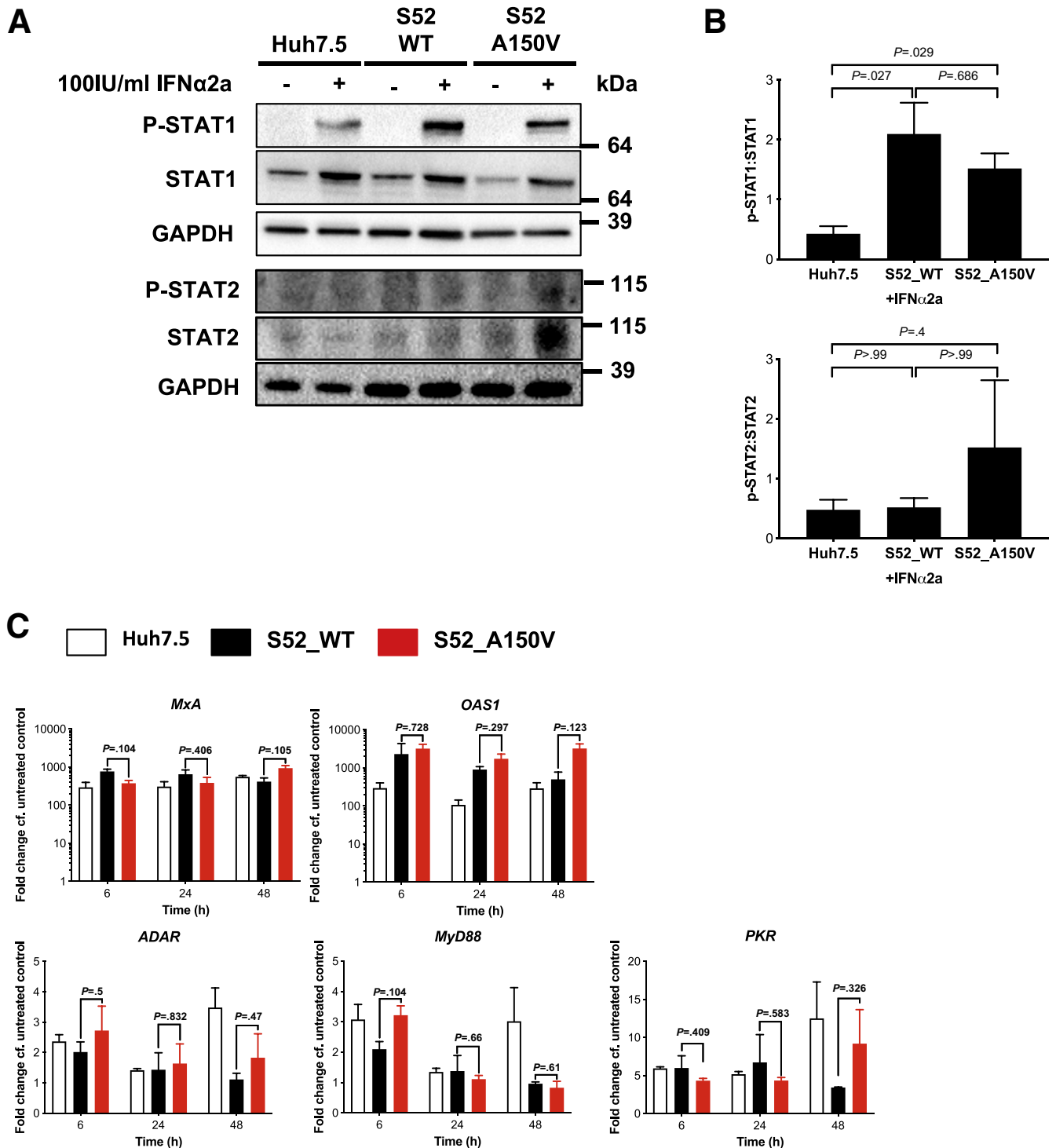

Figure 2. HCV NS5B A150V polymorphism has no effect on IFN signaling and ISG transcriptional activation. (A) Immunoblotting and (B) densitometry analyses of STAT1 and STAT2 phosphorylation in Huh7.5-SEC14L2 cells with stable expression of HCV G3 replicons treated with 100 IU/mL IFNα2a for 6 hours. (C) Expression of ISGs driven by ISGF3 (MxA and OAS1) and unphosphorylated ISGF3 (ADAR, MyD88, and PKR) in Huh7.5-SEC14L2 cells with stable expression of HCV G3 replicons was analyzed by RT-qPCR at 6, 24, and 48 hours after treatment with 100 IU/mL IFNα2a. Data show mean + SEM fold induction normalized to untreated control from at least 3 independent experiments and were analyzed by Mann-Whitney test.
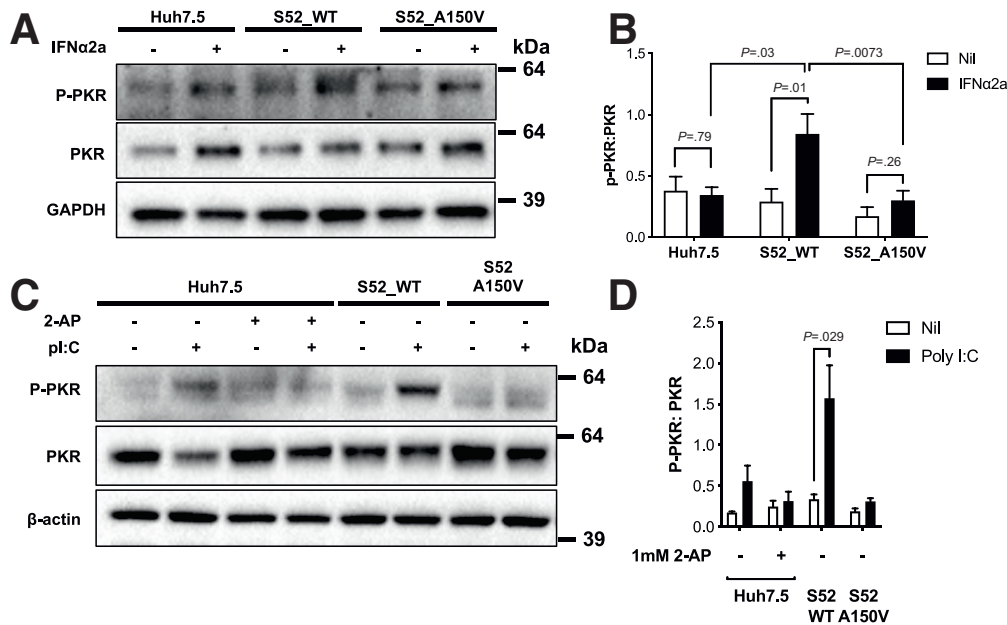
Figure 3. A150V polymorphism reduces PKR phosphorylation in response to IFN. (*A*) Phosphorylated (pT446) and total PKR expression in Huh7.5-SEC14L2 S52 replicon cells was analyzed by immunoblotting 6 hours after treatment with 100 IU/mL IFNα2a. (*B* and *D*) Densitometry analysis of 3 independent experiments showing mean + SEM of ratio of P-PKR: total PKR, and indicated differences in mean were analyzed by Mann-Whitney test. (*C*) 2×10^5 parental Huh7.5-SEC14L2 cells with stable expression of S52 WT or A150V replicons were pretreated with PKR inhibitor 1 mmol/L 2-AP for 1 hour and then treated with 500 ng/mL poly-I:C for 24 hours. Expression of phosphorylated (pT446) PKR and total PKR were analyzed by immunoblotting. Data show representative results from 3 independent experiments.
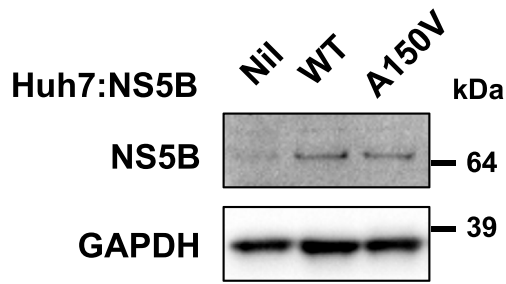
slightly higher than in WT replicon but was decreased upon stimulation in both immunoblotting and quantitative immunofluorescence experiments. In cells containing WT replicons, analysis of the subcellular distribution of phospho-PKR showed increased nuclear localization after IFN stimulation, as previously described[29–31] (Figure 4*C* *lower panel* and *F*). The cytoplasmic level of phospho-PKR in A150V replicon cells was noted to be higher than that in WT replicon cells (Figure 4*C* and *E*). However, after IFN treatment of A150V replicon cells, phospho-PKR remained within the cytoplasm (Figure 4*C* *lower panel* and *E*), where it localized with replicating virus (NS5A; Figure 4*C* *lower panel* and *F*). These data suggest that the A150V polymorphism within NS5B perturbs nuclear translocation of phospho-PKR, which may be retained within the viral replication complex.

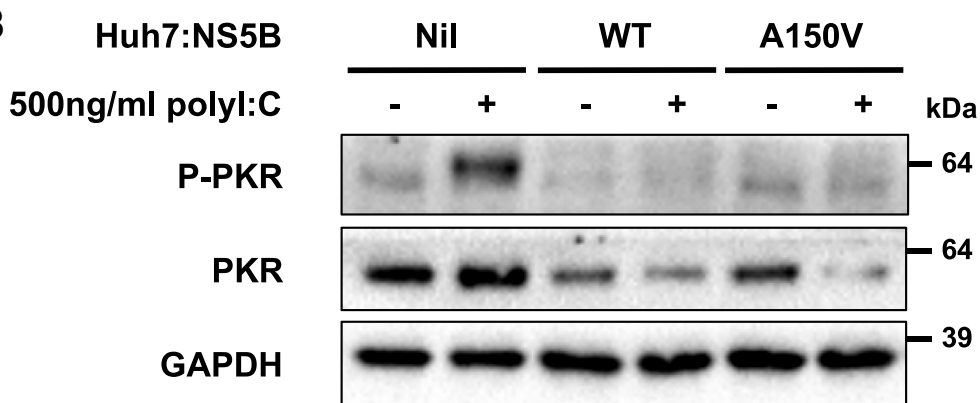## IFN Inhibits Viral Replication via PKR, Inducing Apoptosis in Cells Containing HCV Replicons

To test whether IFN-mediated PKR activation is required for its antiviral effect against HCV, we measured luciferase activity in replicons pretreated with a PKR-specific inhibitor 2-AP, followed by IFN treatment. 2-AP inhibited IFN-mediated PKR activation in WT replicon–expressing cells, whereas, as expected, it had no effect on PKR activation in parental Huh7.5 and A150V replicon–expressing cells (Figure 5*Ai*). Pretreatment of WT replicon–expressing cells with 2-AP to inhibit PKR resulted

in higher luciferase activity (Figure 5*Bi*), suggesting that phospho-PKR may reduce viral replication, although IFN was still able to inhibit viral replication, suggesting that other mechanisms are likely to be involved. Inhibiting PKR activation had no effect on A150V replicon–expressing cells (Figure 5*Bii*), suggesting that this enzyme is not active in these cells. We also examined the effect of enforced activation of PKR on HCV replication. The geldanamycin analogue, 17-AAG, a HSP90 inhibitor, which activates PKR by facilitating dimerization and autophosphorylation,[32] was added to IFN-treated replicon-expressing cells to enhance PKR activation in A150V replicon–expressing cells (Figure 5*C*). Because folding of PKR in the endoplasmic reticulum requires HSP90 and p23,[32] 17-AAG was added 6 hours after IFN (Figure 5*C*) (when higher total PKR level was observed after IFN treatment) to ensure it did not affect de novo synthesis of PKR. Increasing concentrations of 17-AAG alone had antiviral activity in both WT and A150V replicon cells (blue curve compared with 100 IU/mL IFN only in black dotted curve in Figure 5*Di* and *ii*, respectively). Although A150V replicon–expressing cells did not respond to IFN (black dotted curve in Figure 5*Dii*), post-treatment with increasing concentrations of 17-AAG sensitized them to IFN-mediated antiviral effect (red curve compared with black dotted curve; Figure 5*Dii* insert shows antiviral effect at 32 nmol/L 17-AAG, the same concentration used in Figure 5*C*). Collectively, these data suggest that PKR activation is required for IFN-mediated antiviral activity in WT
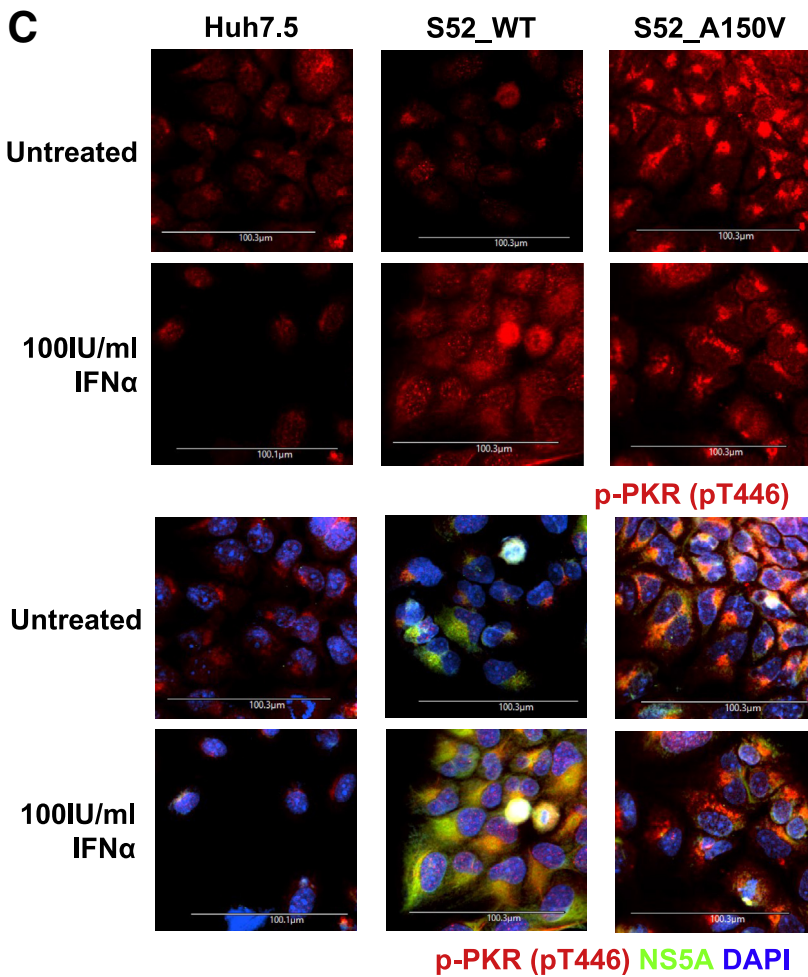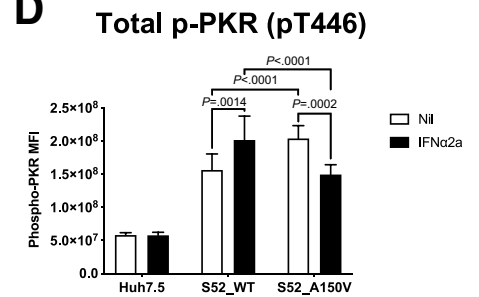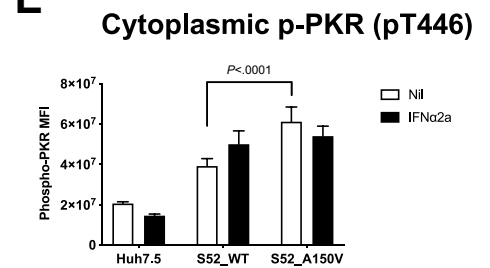
A

B

C
p-PKR (pT446)

p-PKR (pT446) NS5A DAPI

D Total p-PKR (pT446)
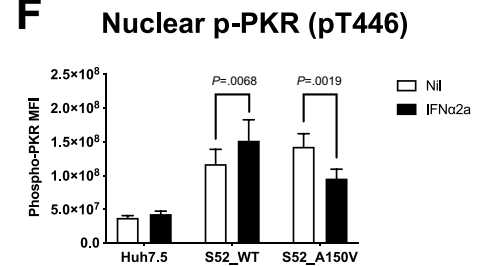
E Cytoplasmic p-PKR (pT446)

F Nuclear p-PKR (pT446)

replicon–expressing cells, and A150V replicon blocks this activity, although the replicon remains sensitive to PKR activation induced by other means.

IFN-induced nuclear localization of PKR[29,33] is associated with induction of apoptosis.[34,35] Treatment of WT replicon cells with IFN alpha for 24 hours led to an increase in cell death, whereas IFN had no effect on cells with stable expression of A150V replicon (Figure 6A). As expected, cells that did not express the replicon and lacked viral RNA did not phosphorylate PKR and were unaffected by IFN. Using antibodies specific for cleaved caspase 3, a phenotypic marker for apoptosis, we showed that the increased proportion of cell death in WT replicon–expressing cells was due to apoptosis (Figure 6B). The pro-apoptotic phenotype induced by IFN in WT replicon–expressing cells was independent of endoplasmic reticulum stress because IFN did not change the level of activated PERK (Figure 6C). Because IFN also did not change the level of activated RIP3 and LC3B, markers for necrosis and autophagy, respectively (Figure 6D and E), the increased level of cell death in WT replicon–expressing cells was attributed to induction of apoptosis. To understand whether PKR activation contributes to increased rate of apoptosis, we analyzed the induction of cell death in cells pretreated with a PKR-specific inhibitor, 2-AP, after IFN treatment. Pretreatment of 2-AP reduced the level of PKR activation (Figure 5A) and reduced concomitant cell death in IFN-treated WT replicon–expressing cells (blue vs black bars of WT replicons in Figure 6A). On the contrary, enforced activation of PKR by 17-AAG after IFN treatment (Figure 5C) led to increased level of cell death in replicon-expressing cells (red bars in Figure 6A for both WT and A150V replicons).

Discussion

Type I IFNs establish an antiviral state via transcriptional activation of ISGs that promote an antiviral intracellular landscape. In this study, we show how a polymorphism in NS5B, A150V of G3 HCV counteracts IFN by inhibiting PKR activity. Using a subgenomic replicon system and virally infected cells, we demonstrated that the A150V polymorphism confers resistance to the downstream effects of IFN. Examination of proximal IFN signaling did not reveal any difference between WT and A150V replicons, and IFN-driven up-regulation of ISGs is intact in A150V. These data indicate that this polymorphism in NS5B has no effect on the signaling cascade leading to ISG induction. Because PKR, an IFN-inducible antiviral protein, has been implicated in control of HCV replication and it has recently been shown to mediate cyclophilin A–dependent antiviral activity of G2 HCV in vitro,[36] we sought to understand whether PKR activation is

altered in replicon-expressing cells. Our immunoblotting and immunofluorescence results highlight that PKR activation and nuclear localization of activated PKR are inhibited by NS5B with the A150V polymorphism. Because activation of PKR by IFN-independent mechanisms reduces HCV A150V RNA replication and inhibition of PKR enhances HCV RNA replication in WT replicon cells, we conclude that the effect of the A150V polymorphism on the antiviral effect of IFN is mediated, at least in part, by inhibition of PKR. Using quantitative immunofluorescence, we show that increased phosphorylated PKR in WT replicon–expressing cells was predominantly localized to the nucleus, whereas there was a decrease in phospho-PKR translocation in A150V replicon–expressing cells. Nuclear localization of activated PKR has been implicated in the onset of cellular stress at the endoplasmic reticulum,[29] and this results in the induction of apoptosis.[34] Whereas IFN increased the rate of apoptosis in WT replicon–expressing cells, this was reduced in cells expressing the A150V polymorphism. Because inhibition of PKR activation with 2-AP rescued IFN-treated WT replicons from cell death, our data suggest that the A150V polymorphism exerts its inhibitory effect on the induction of cellular apoptosis by interfering with PKR activation.

The mechanism by which the A150V polymorphism of NS5B inhibits PKR activation is not yet fully characterized. Because high level expression of WT NS5B inhibits PKR activation and because structural modeling of the NS5B A150 residue reveals that it is within the interaction interface with the NS5A protein of HCV,[16] which sequesters replicating viral proteins on the endoplasmic reticulum, we speculate that changes to the association of NS5A and NS5B may lead to enhanced expression of non-virally associated NS5B leading to PKR inhibition. This hypothesis is supported by our immunofluorescence data showing differences in the localization of PKR and replicating HCV in cells containing the NS5B A150V polymorphism, but further studies using labelled viral proteins will be required to confirm this hypothesis, and these studies are underway.

The strength of this work is that it provides a detailed analysis of the impact of a G3 polymorphism on the antiviral effects of IFN. The association between a polymorphism that reduces the effectiveness of sofosbuvir and IFN may provide a mechanism to explain why patients with G3 HCV who have failed to respond to a course of IFN therapy respond less well to sofosbuvir-based regimens. The observation that a viral polymorphism may modify cellular apoptosis leads to speculation that this polymorphism may be involved in malignant transformation, and sequencing studies to examine this possibility are under way.

Figure 4. (*See previous page*). **A150V NS5B altered co-localization of NS5A and phospho-PKR in response to IFN.** (*A*) Huh7 cells with stable expression of WT and A150V NS5B. (*B*) Huh7 cells with stable expression of WT or A150V NS5B were treated with 500 ng/mL poly I:C for 24 hours. Phosphorylation of PKR and total PKR were analyzed by immunoblotting. (*C*) Quantitative immunofluorescence of PKR (pT446) phosphorylation (*red*) in Huh7.5-SEC14L2 cells with stable expression of HCV G3 replicons, represented by NS5A (*green*), treated with 100 IU/mL IFNα2a for 6 hours; DAPI (*blue*) was used to label DNA. Immunofluorescence intensity of phosphorylated PKR in (*D*) whole cell, (*E*) cytoplasm, and (*F*) nuclei was quantified on a per cell basis. Data show mean + SEM from 3 independent experiments and were analyzed by Wilcoxon signed-rank test. MFI, mean fluorescent intensity.
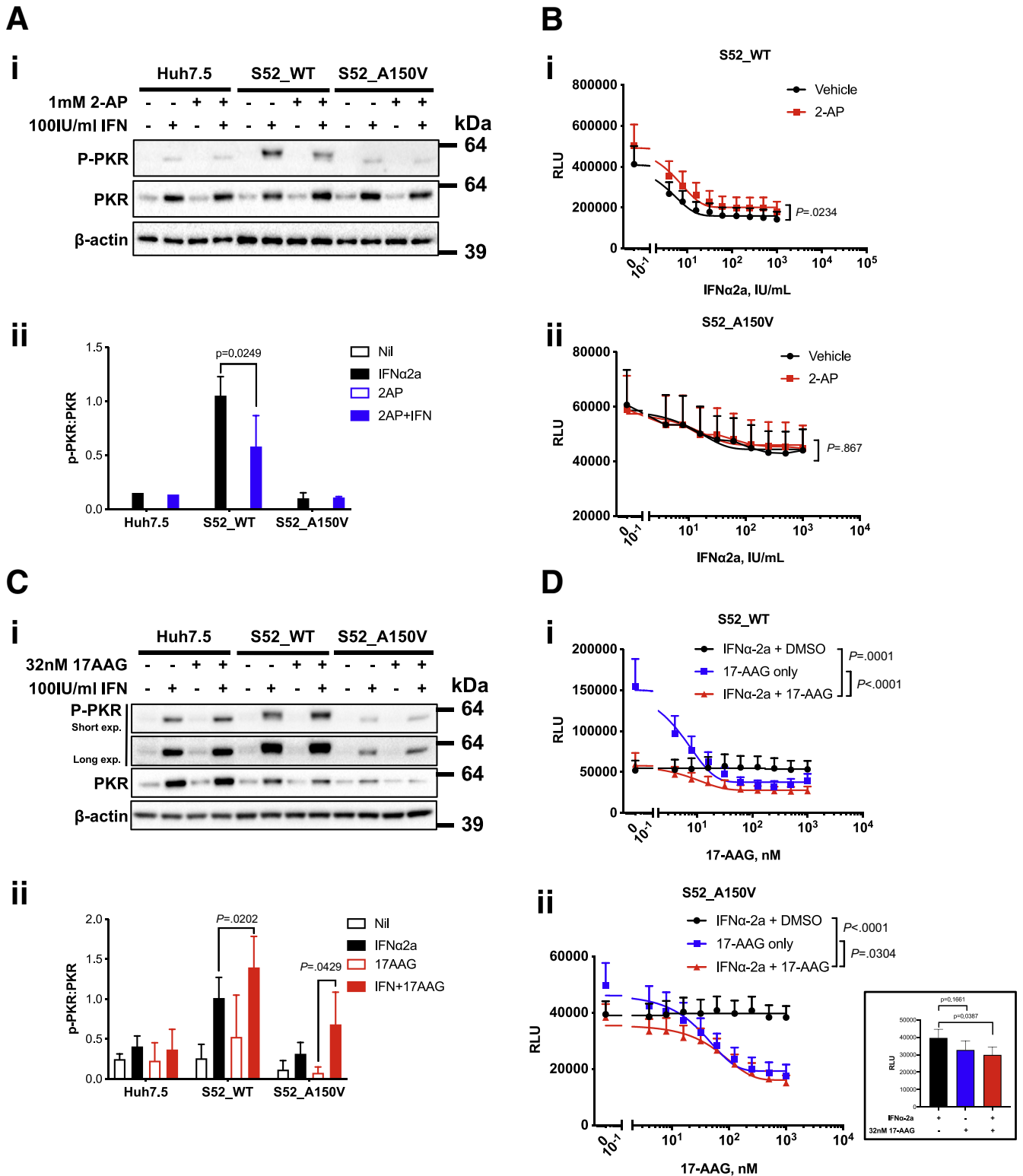
Figure 5. PKR activity potentiates viral replication in response to IFN. Huh7.5-SEC1L2 parental and WT/A150V replicon–expressing cells were pretreated with vehicle control (PBS-acetic acid, 200:1 v/v) or 1 mmol/L 2-AP and then treated with a dilution series of IFNα2a for 24 hours before analysis of (*A*) level of phospho/total PKR by (*i*) immunoblotting and (*ii*) densitometry and (*B*) analyses of viral replication by luciferase activity assay. WT/A150V replicon–expressing cells were treated with or without 100 IU/mL IFNα2a for 6 hours before addition of vehicle control (dimethyl sulfoxide) or 17-AAG. (*C*) Phospho/total PKR levels were analyzed by (*i*) immunoblotting and (*ii*) densitometry; (*D*) viral replication was analyzed by luciferase activity assay; *insert* shows luciferase activity in cells treated with or without IFNα2a and 32 nmol/L 17-AAG. Data show mean + SEM from at least 3 independent experiments; indicated differences in mean were analyzed by paired Student *t* test in (*Aii*), (*Cii*), and (*Dii insert*) and 2-way analysis of variance in (*B*) and (*D*). RLU, relative light unit.
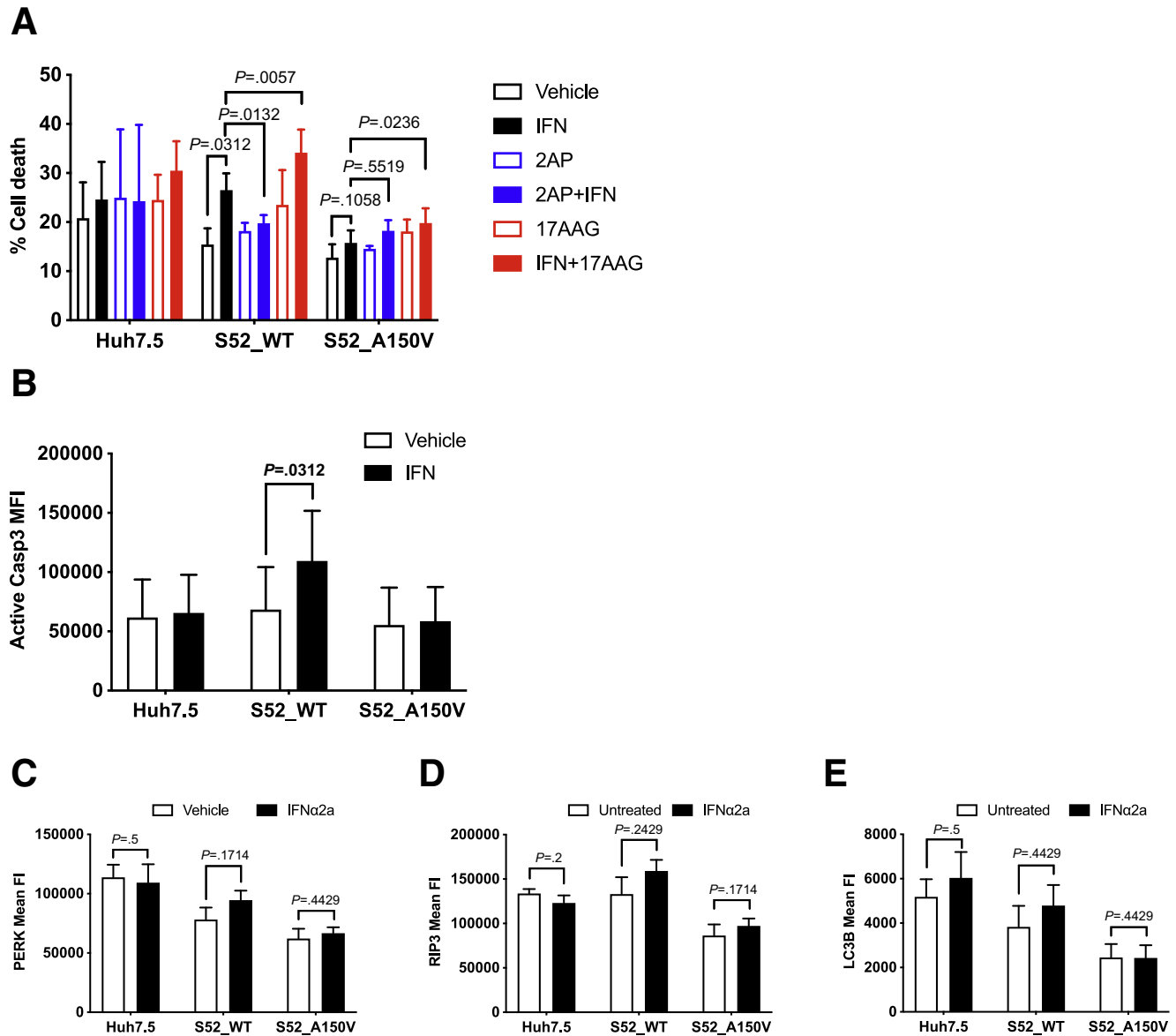
A

B

C

D

E

Figure 6. IFN-mediated PKR activation induces apoptosis-mediated cell death in replicon cells. Huh7.5-SEC1L2 parental and WT/A150V replicon–expressing cells were pretreated with vehicle control or 1 mmol/L 2-AP and then treated with 100 IU/mL IFN for 24 hours, or pretreated with IFN for 6 hours and then 32 mmol/L 17-AAG for 18 hours before level of cell death was measured by (A) Zombie NIR dye for total cell death followed by fixation, intracellular staining of (B) active caspase 3, (C) PERK, (D) RIP3, (E) LC3B, and flow cytometry. Data show mean + SEM from at least 3 independent experiments, and indicated differences in mean were analyzed by Wilcoxon signed-rank test.

In summary, our work provides a detailed analysis of the impact of a G3 polymorphism on the antiviral effects of IFN, demonstrating a novel modulation of the innate antiviral response mediated by the HCV NS5B.

Materials and Methods

Cells, Reagents, and Viruses

Huh7 and Huh7.5-SEC14L2 cells (gift from P. Simmonds, Oxford) were propagated in Dulbecco modified Eagle medium (DMEM) supplemented with 10% heat-inactivated fetal calf serum, 100 U/mL streptomycin, 100 U/mL penicillin, and 2 mmol/L L-glutamine (all from Thermo Fisher, Waltham, MA). Huh7.5-SEC14L2 cells expressing HCV G3 S52 WT and A150V replicon[25] were maintained in the presence of 750 μg/mL G418 (Sigma-Aldrich, St Louis, MO). 2-AP is from Sigma-Aldrich. IFNα2a was from Pepro-Tech (Rocky Hill, NJ), and sofosbuvir was provided by Gilead Sciences, Foster City, CA. Polyinosinic-polycytidylic acid (1:6 w/w, high molecular weight, 1.5–8 kb) conjugated with LyoVec and 17-(allylamino)-17-demethoxygeldanamycin (17-AAG) are from InvivoGen (San Diego, CA).

Infectious G3 cell-culture-derived HCV was generated as detailed previously.[16]

Quantification of HCV Foci Using INCell Automated Microscope

Huh7.5-SEC14L2 cells were seeded at 3×10^3 cells/well in 96-well plates for 24 hours before infection with 1:3 serial dilutions of supernatants from cells producing DBN WT or A150V viruses for 4 days. Cells were then washed in phosphate-buffered saline (PBS), fixed with ice-cold methanol, blocked in 3% fetal calf serum/PBS, and incubated with sheep polyclonal anti-NS5A (donation from Prof Mark Harris) diluted at 1:1000 for 1 hour at room temperature. After incubation with 1:1000 AlexaFluor 488 conjugated anti-sheep immunoglobulin G for 1 hour at room temperature and washes with PBS, plasma membrane was labelled with 1:1000 HCS Cell Mask Deep Red Stain (Invitrogen, Carlsbad, CA) for 1.5 hours. HCV foci were quantified with GE High-throughput INCA2200 automated microscope (GE Healthcare, Chicago, IL) with 9 fields/well using a $\times 20$ objective. Images were analyzed by using the high content analysis software developer toolbox (GE, v. 1.9.2). Raw images were processed to define nuclear and cytoplasmic borders on the basis of DAPI and cell mask staining. NS5A-positive cells are defined as infected cells, and percentage of infection was calculated as percentage of infected cells in all nucleated cells with defined nuclear and cytoplasmic staining.

Quantitative PCR Measurement of ISGs and HCV RNA

Huh7 (and its NS5B-expressing lines) and Huh7.5-SEC14L2 replicon cells were plated in 6-well plates at $2 \times 10^4/cm^2$ 12–14 hours before experiments. Medium was replaced with 2% heat-inactivated fetal calf serum–containing DMEM for 2 hours and then left untreated or treated with 100 IU/mL IFNα2a for indicated durations. RNA was purified using RNeasy mini kit (Qiagen, Hilden, Germany). After DNA removal with RQ1 DNase kit (Promega, Madison, WI), 1 μg RNA was reverse transcribed into cDNA with random primers and GoScript reverse transcription kit (Promega) according to manufacturer's instructions. Five hundred ng cDNA was used for qPCR in AB1 7500 (ABI Biosystem) using SYBR Green (Thermo Fisher) and the following primers (all shown in 5′ to 3′): MxA, forward, AACAACCTGTGCAGCCAGTA, reverse, AAGGGCAACTCCTGAGAGTG; OAS1, forward, TGAGGTCCAGGCTCCACGCT, reverse, GCAGGTCGGTGCACTCCTCG; ADAR, forward, ACCTGAACACCAACCCTGTG, reverse, CGACCCCCAACTTTTGCTTG; MyD88, forward, GTCTGACCGCGATGTCCTGCC, reverse, ACAACCACCACCATCCGGCG; PKR, forward, TCTCTGGCGGTCTTCAGAAT, reverse, ACTCCCTGCTTCTGACGGTA; 5S, forward, TGTGATTTCCGCTGGTACGG, reverse, AGCCATCTCGAACCAGACAC; HCV, forward, GCGAACCGGTGAGTACAC, reverse, TACCACAAGGCCTTTCGC.

RNA in DBN virus-infected cells was extracted with TRIzol (Invitrogen) and quantified by using RiboGreen (Invitrogen) according to manufacturer's instructions. HCV RNA copy number was quantified by using a 1-step RT-qPCR with the Quantitect Viral Nuclei Acid detection kit (Qiagen) according to manufacturer's instructions. Triplicate samples with a standard curve of known amounts of JFH-1 were analyzed with primers, HCV forward, GCCTTGTGGTACTGCCTG, HCV reverse, CACGGTCTACGAGACCTCC and HCV probe, ATAGGGTGCTTGCGAGTGCCCCGGG, on Rotorgene 60000 (Qiagen). Absolute quantification of HCV RNA was performed by including serial dilutions of an RNA standard in each PCR run and expressed relative to total sample RNA.

Immunoblotting

Cells were washed once with PBS and then lyzed in radioimmunoprecipitation buffer (containing 20 mmol/L Tris pH 7.5, 150 mmol/L NaCl, 1 mmol/L EDTA, 1 mmol/L EGTA, 1% NP40, 1% sodium deoxycholate, 250 μmol/L sodium pyrophosphate, 1 mmol/L β-glycerophosphate, 1 mmol/L sodium vanadate and protease inhibitor cocktail, all from Sigma-Aldrich) for 30 minutes at 4°C. Lysate was then centrifuged for 15,000g for 10 minutes at 4°C. Protein concentration of supernatant was determined by bicinchoninic acid assay (Thermo Fisher). Ten μg of protein per sample was analyzed by immunoblotting, developed with ECL Prime reagents (GE Healthcare Life Sciences), and captured with ChemiDoc MP system (Bio-Rad, Hercules, CA). Intensity of immunobands was analyzed with ImageLab (Bio-Rad). Rabbit monoclonal anti-phospho-STAT1 (Y701, clone D4A7; Cell Signaling Technology, Danvers, MA), rabbit polyclonal anti-STAT1 (9172; Cell Signaling Technology), rabbit polyclonal anti-phospho-STAT2 (Y689; Upstate, Greenville, SC), mouse monoclonal anti-STAT2 (clone 22/Stat2; BD Biosciences, Franklin, NJ), rabbit monoclonal anti-phospho-PKR (pT446, clone E120; Abcam, Cambridge, UK), rabbit monoclonal anti-PKR (clone YE350; Abcam), and rabbit polyclonal anti-HCV NS5B (ab65410; Abcam) were used at 1:1000, and secondary antibodies, horseradish peroxidase–conjugated goat anti-rabbit/mouse immunoglobulin G (Santa Cruz Biotechnology, Dallas, TX), were used at 1:10,000.

Quantitative Immunofluorescence

Cells were plated onto glass cover slips at $1 \times 10^4/cm^2$ 12–14 hours before experiment, cells were treated with 2% heat-inactivated fetal calf serum supplemented DMEM for 2 hours and then treated with 100 IU/mL IFNα2a for 6 hours. Cells were then washed with PBS, fixed in ice-cold methanol at –20°C for 20 minutes, and then washed in PBS. Fixed cells were then permeabilized in 0.2% (v/v) Triton X-100 in PBS for 20 minutes and then blocked in 4% bovine serum albumin, 0.1% (v/v) Triton X100 in PBS for 1 hour at room temperature. Primary antibodies, including sheep polyclonal anti-NS5A (gift from Prof Mark Harris), were diluted in staining buffer (0.1% Triton-X100, 2% bovine serum albumin in PBS) at 1:100, and cells were incubated overnight at 4°C. Secondary antibodies used were donkey anti-rabbit conjugated with Alexa-Fluor 647 and donkey anti-sheep conjugated with Alexa-Fluor 488 (for NS5A detection) were diluted in staining buffer at 1:250, and cells were incubated for 1 hour at room temperature. After 3 successive washes with PBS, cells were counterstained with blue cell mask (1:1000; BM-1) and 2 μg/mL DAPI (both from ChemoMetec, Lillerød, Denmark) in PBS for 30 minutes at room temperature. Cover slips were then mounted onto

glass microscopic slides with ProLong Diamond anti-fade mount overnight at room temperature. Imaging was performed with XCyto 10 imager with XCyto Cell Viewer at $20\times$ magnification (ChemoMetec). Cells were exposed for 400 ms with excitation lasers LED405 (for DAPI and blue cell mask), LED488 (for Alexa Fluor 488), and LED635 (for Alexa Fluor 647). Band pass filters used were DAPI, 573-613; cell mask, 430-475; Alexa Fluor 488, 513-555; and Alexa Fluor 647, 665-705. Images were screened to gate out debris and non-focused images. Data were then converted to FCS files to be further processed with Flow Jo version 10 (BD).

Flow Cytometry and Data Analysis

Huh7.5-SEC14L2 cells with and without stable expression of WT and A150V replicons were plated at $2 \times 10^4/$ cm^2 in 6-well plate 12–14 hours before experiments. After 24-hour treatment with 100 IU/mL IFN, cells were trypsinized and washed in PBS before intracellular staining modified.[37] Zombie-NIR dead cell dye (1:1000 diluted in PBS; BioLegend, San Diego, CA) was used to label dead cells at room temperature for 15 minutes in the dark. Cells were then washed once in PBS, resuspended in Fix/Perm buffer A (Caltag Medsytems, Buckingham, UK), and incubated at room temperature for 20 minutes. Cells were then permeabilized in 0.25% Triton X-100/PBS for 20 minutes at room temperature before immunolabeling with anti-LC3B monoclonal antibody (1:400; Cell Signaling Technology) for 20 minutes at room temperature. Washed cells were then labeled with Alexa-Fluor 647–conjugated anti-rabbit immunoglobulin G (Invitrogen) for 20 minutes at room temperature. Cells were then washed and labeled with anti-PERK-AF488 (1:100), RIP3-phycoerythrin (PE) (clone B-2; Santa Cruz Biotechnology), PARP-PE-CF595, H2AX-PE-Cy7, and anti-active caspase 3-BV650 for 20 minutes at room temperature. Washed cells were resuspended in 300 μL PBS and analyzed on a ACEA Bioscience (San Diego, CA) Novocyte 3000 flow cytometer with an acquisition of 100,000 events. LC3B-AF647 and Zombie-NIR were excited by the 633 nm laser and collected at 675/30 nm and 780/60 nm detectors, respectively. Caspase 3-BV650 was excited by the 405 nm laser and collected at 675/30 nm. PERK-AF488, RIP-PE, PARP-PE-CF595, and H2AX-PE-Cy7 were excited by the 488 nm laser and collected at 530/30, 572/28, 615/20, and 780/60 nm filters, respectively. Single color controls were used to determine color compensation by using the pre-set voltages on the instrument using Novo Express software (ver. 1,2,5; ACEA Biosciences). Cells were first gated on forward scatter (FSC) vs side scatter minus debris and then on a FSC-W vs FSC-H dot plot for single cell events before further analysis in fluorescence intensity of indicated markers.

Statistical Analysis

All data show mean + standard error of the mean (SEM) or representative result from at least 3 independent experiments. Statistical analyses were performed with Prism 8 (GraphPad, San Diego, CA).

References

1. GBD 2016 Disease and Injury Incidence and Prevalence Collaborators. Global, regional, and national incidence, prevalence, and years lived with disability for 328 diseases and injuries for 195 countries, 1990-2016: a systematic analysis for the Global Burden of Disease Study 2016. Lancet 2017;390:1211–1259.

2. D'Souza R, Foster GR. Diagnosis and treatment of hepatitis C. J R Soc Med 2004;97:223–225.

3. Foster GR, Afdhal N, Roberts SK, Bräu N, Gane EJ, Pianko S, Lawitz E, Thompson A, Shiffman ML, Cooper C, Towner WJ, Conway B, Ruane P, Bourlière M, Asselah T, Berg T, Zeuzem S, Rosenberg W, Agarwal K, Stedman CAM, Mo H, Dvory-Sobol H, Han L, Wang J, McNally J, Osinusi A, Brainard DM, McHutchison JG, Mazzotta F, Tran TT, Gordon SC, Patel K, Reau N, Mangia A, Sulkowski M. ASTRAL-2 Investigators, ASTRAL-3 Investigators. Sofosbuvir and velpatasvir for HCV genotype 2 and 3 infection. N Engl J Med 2015; 373:2608–2617.

4. Curry MP, O'Leary JG, Bzowej N, Muir AJ, Korenblat KM, Fenkel JM, Reddy KR, Lawitz E, Flamm SL, Schiano T, Teperman L, Fontana R, Schiff E, Fried M, Doehle B, An D, McNally J, Osinusi A, Brainard DM, McHutchison JG, Brown RS, Charlton M. ASTRAL-4 Investigators. Sofosbuvir and velpatasvir for HCV in patients with decompensated cirrhosis. N Engl J Med 2015; 373:2618–2628.

5. Zein NN, Rakela J, Krawitt EL, Reddy KR, Tominaga T, Persing DH. Hepatitis C virus genotypes in the United States: epidemiology, pathogenicity, and response to interferon therapy—Collaborative Study Group. Ann Intern Med 1996;125:634–639.

6. McHutchison JG, Gordon SC, Schiff ER, Shiffman ML, Lee WM, Rustgi VK, Goodman ZD, Ling MH, Cort S, Albrecht JK. Interferon alfa-2b alone or in combination with ribavirin as initial treatment for chronic hepatitis C: Hepatitis Interventional Therapy Group. N Engl J Med 1998;339:1485–1492.

7. Fried MW, Shiffman ML, Reddy KR, Smith C, Marinos G, Gonçales FL, Häussinger D, Diago M, Carosi G, Dhumeaux D, Craxi A, Lin A, Hoffman J, Yu J. Peginterferon alfa-2a plus ribavirin for chronic hepatitis C virus infection. N Engl J Med 2002;347:975–982.

8. Miglioresi L, Bacosi M, Russo F, Patrizi F, Saccenti P, Ursitti A, Angelis AD, Ricci GL. Consensus interferon versus interferon-alpha 2b plus ribavirin in patients with relapsing HCV infection. Hepatol Res 2003; 27:253–259.

9. Hadziyannis SJ, Sette H, Morgan TR, Balan V, Diago M, Marcellin P, Ramadori G, Bodenheimer H, Bernstein D, Rizzetto M, Zeuzem S, Pockros PJ, Lin A, Ackrill AM; PEGASYS International Study Group. Peginterferon-alpha2a and ribavirin combination therapy in chronic hepatitis C: a randomized study of treatment duration and ribavirin dose. Ann Intern Med 2004;140:346–355.

10. Sjogren MH, Sjogren R, Lyons MF, Ryan M, Santoro J, Smith C, Reddy KR, Bonkovsky H, Huntley B, Faris-

Young S. Antiviral response of HCV genotype 1 to consensus interferon and ribavirin versus pegylated interferon and ribavirin. Dig Dis Sci 2007;52:1540–1547.

11. Chao DT, Abe K, Nguyen MH. Systematic review: epidemiology of hepatitis C genotype 6 and its management. Aliment Pharmacol Ther 2011;34:286–296.

12. Shoeb D, Rowe IA, Freshwater D, Mutimer D, Brown A, Moreea S, Sood R, Marley R, Sabin CA, Foster GR. Response to antiviral therapy in patients with genotype 3 chronic hepatitis C: fibrosis but not race encourages relapse. Eur J Gastroenterol Hepatol 2011;23:747–753.

13. Bourlière M, Gordon SC, Flamm SL, Cooper CL, Ramji A, Tong M, Ravendhran N, Vierling JM, Tran TT, Pianko S, Bansal MB, de Lédinghen V, Hyland RH, Stamm LM, Dvory-Sobol H, Svarovskaia E, Zhang J, Huang KC, Subramanian GM, Brainard DM, McHutchison JG, Verna EC, Buggisch P, Landis CS, Younes ZH, Curry MP, Strasser SI, Schiff ER, Reddy KR, Manns MP, Kowdley KV, Zeuzem S. POLARIS-1 and POLARIS-4 Investigators. Sofosbuvir, velpatasvir, and voxilaprevir for previously treated HCV infection. N Engl J Med 2017; 376:2134–2146.

14. European Association for the Study of the Liver. Electronic address: easloffice@easloffice.eu & European Association for the Study of the Liver—EASL recommendations on treatment of hepatitis C 2018. J Hepatol 2018;69:461–511.

15. Ansari MA, Pedergnana V, Ip C, Magri A, Von Delft A, Bonsall D, Chaturvedi N, Bartha I, Smith D, Nicholson G, McVean G, Trebes A, Piazza P, Fellay J, Cooke G, Foster GR, STOP-HCV Consortium, Hudson E, McLauchlan J, Simmonds P, Bowden R, Klenerman P, Barnes E, Spencer CCA. Genome-to-genome analysis highlights the effect of the human innate and adaptive immune systems on the hepatitis C virus. Nat Genet 2017;49:666–673.

16. Wing PAC, Jones M, Cheung M, DaSilva S, Bamford C, Jason Lee W-Y, Aranday-Cortes E, Da Silva Filipe A, McLauchlan J, Smith D, Irving W, Cunningham M, Ansari A, Barnes E, Foster GR. Amino acid substitutions in genotype 3a hepatitis C virus polymerase protein affect responses to sofosbuvir. Gastroenterology 2019; 157:692–704.e9.

17. Wong M-T, Chen SS-L. Emerging roles of interferon-stimulated genes in the innate immune response to hepatitis C virus infection. Cell Mol Immunol 2016; 13:11–35.

18. García MA, Gil J, Ventoso I, Guerra S, Domingo E, Rivas C, Esteban M. Impact of protein kinase PKR in cell biology: from antiviral to antiproliferative action. Microbiol Mol Biol Rev 2006;70:1032–1060.

19. Knapp S, Yee LJ, Frodsham AJ, Hennig BJW, Hellier S, Zhang L, Wright M, Chiaramonte M, Graves M, Thomas HC, Hill AVS, Thursz MR. Polymorphisms in interferon-induced genes and the outcome of hepatitis C virus infection: roles of MxA, OAS-1 and PKR. Genes Immun 2003;4:411–419.

20. Shimoike T, McKenna SA, Lindhout DA, Puglisi JD. Translational insensitivity to potent activation of PKR by HCV IRES RNA. Antiviral Res 2009;83:228–237.

21. Gale M, Blakely CM, Kwieciszewski B, Tan SL, Dossett M, Tang NM, Korth MJ, Polyak SJ, Gretch DR, Katze MG. Control of PKR protein kinase by hepatitis C virus nonstructural 5A protein: molecular mechanisms of kinase regulation. Mol Cell Biol 1998; 18:5208–5218.

22. Pflugheber J, Fredericksen B, Sumpter R, Wang C, Ware F, Sodora DL, Gale M. Regulation of PKR and IRF-1 during hepatitis C virus RNA replication. Proc Natl Acad Sci USA 2002;99:4650–4655.

23. Wang C, Pflugheber J, Sumpter R, Sodora DL, Hui D, Sen GC, Gale M. Alpha interferon induces distinct translational control programs to suppress hepatitis C virus RNA replication. J Virol 2003;77:3898–3912.

24. Suzuki R, Matsuda M, Shimoike T, Watashi K, Aizaki H, Kato T, Suzuki T, Muramatsu M, Wakita T. Activation of protein kinase R by hepatitis C virus RNA-dependent RNA polymerase. Virology 2019;529:226–233.

25. Ramirez S, Mikkelsen LS, Gottwein JM, Bukh J. Robust HCV genotype 3a infectious cell culture system permits identification of escape variants with resistance to sofosbuvir. Gastroenterology 2016;151:973–985.e2.

26. Sung PS, Cheon H, Cho CH, Hong S-H, Park DY, Seo H-I, Park S-H, Yoon SK, Stark GR, Shin E-C. Roles of unphosphorylated ISGF3 in HCV infection and interferon responsiveness. Proc Natl Acad Sci USA 2015; 112:10443–10448.

27. Dey M, Mann BR, Anshu A, Mannan MA. Activation of protein kinase PKR requires dimerization-induced cis-phosphorylation within the activation loop. J Biol Chem 2014;289:5747–5757.

28. Balachandran S, Roberts PC, Brown LE, Truong H, Pattnaik AK, Archer DR, Barber GN. Essential role for the dsRNA-dependent protein kinase PKR in innate immunity to viral infection. Immunity 2000;13:129–141.

29. Jeffrey IW, Kadereit S, Meurs EF, Metzger T, Bachmann M, Schwemmle M, Hovanessian AG, Clemens MJ. Nuclear localization of the interferon-inducible protein kinase PKR in human cells and transfected mouse cells. Exp Cell Res 1995;218:17–27.

30. Kim Y, Lee JH, Park J-E, Cho J, Yi H, Kim VN. PKR is activated by cellular dsRNAs during mitosis and acts as a mitotic regulator. Genes Dev 2014;28:1310–1322.

31. Maarifi G, El Asmi F, Maroui MA, Dianoux L, Chelbi-Alix MK. Differential effects of SUMO1 and SUMO3 on PKR activation and stability. Sci Rep 2018;8:1277.

32. Donzé O, Abbas-Terki T, Picard D. The Hsp90 chaperone complex is both a facilitator and a repressor of the dsRNA-dependent kinase PKR. EMBO J 2001; 20:3771–3780.

33. Besse S, Rebouillat D, Marié I, Puvion-Dutilleul F, Hovanessian AG. Ultrastructural localization of interferon-inducible double-stranded RNA-activated enzymes in human cells. Exp Cell Res 1998;239:379–392.

34. Onuki R, Bando Y, Suyama E, Katayama T, Kawasaki H, Baba T, Tohyama M, Taira K. An RNA-dependent protein kinase is involved in tunicamycin-induced apoptosis and Alzheimer's disease. EMBO J 2004;23:959–968.

35. Lee E-S, Yoon C-H, Kim Y-S, Bae Y-S. The double-strand RNA-dependent protein kinase PKR plays a

significant role in a sustained ER stress-induced apoptosis. FEBS Lett 2007;581:4325–4332.

36. Colpitts CC, Ridewood S, Schneiderman B, Warne J, Tabata K, Ng CF, Bartenschlager R, Selwood DL, Towers GJ. Hepatitis C virus exploits cyclophilin A to evade PKR. Elife 2020;9.

37. Bergamaschi D, Vossenkamper A, Lee WYJ, Wang P, Bochukova E, Warnes G. Simultaneous polychromatic flow cytometric detection of multiple forms of regulated cell death. Apoptosis 2019; 24:453–464.

CRediT Authorship Contributions
Graham R. Foster, FRCP, PhD (Conceptualization: Lead; Funding acquisition: Lead; Resources: Lead; Supervision: Lead; Writing – original draft: Equal)

Wing-Yiu Jason Lee, PhD (Data curation: Lead; Formal analysis: Lead; Investigation: Lead; Methodology: Equal; Project administration: Lead; Validation: Lead; Visualization: Lead; Writing – original draft: Equal; Writing – review & editing: Equal)

Meleri Jones, PhD (Data curation: Supporting; Formal analysis: Supporting; Investigation: Supporting; Methodology: Equal; Project administration: Supporting; Validation: Supporting; Writing – review & editing: Equal)

Peter A. C. Wing, PhD (Data curation: Supporting; Formal analysis: Supporting; Investigation: Supporting; Methodology: Equal; Validation: Supporting; Writing – review & editing: Equal)

Swathi Rajagopal, Dr (Investigation: Supporting; Methodology: Supporting; Writing – review & editing: Equal)